Research Article BEU Fen Bilimleri Dergisi 15(2): 686-695 (2026) DOI: 10.17798/bitlisfen.1817206

BİTLİS EREN UNIVERSITY
FEN BİLİMLERİ DERGİSİ
ISSN: 2147-3129 / e-ISSN: 2147-3188

COMPARISON OF DIFFERENT INFILL PATTERNS IN CYLINDRICAL PLA TENSILE TEST SPECIMENS PRODUCED WITH FDM

Emrah UYSAL

Düzce University, Mechanical Engineering Department, Düzce, Türkiye, emrahuysal@duzce.edu.tr

Article Info

Received: *November 4, 2025*
Revised: *December 14, 2025*
Accepted: *December 15, 2025*

Keywords
FDM,
PLA,
Infill Patterns,
Mechanical Properties,
Shrinkage Ratio.

ABSTRACT

Additive manufacturing technologies have become one of the most studied production methods in recent years thanks to their numerous advantages. The technology, which has spread from home and office environments to industry, increasingly using in many sectors. Among these methods, FDM-type 3D printers are the most preferred additive manufacturing method due to their affordability and ease of application. However, because the polymers used in FDM must be thermoplastic, they are available in a smaller range compared to traditional methods. Furthermore, due to their layered structure, the strength properties of these thermoplastics lower compared to methods such as injection molding. Therefore, studies have focused on optimizing printing parameters that directly affect material development and strength. This study examined infill patterns, which play a critical role in printing parameters. Tensile samples with 11 different patterns were produced using FDM, and their stress and strain values were compared. Furthermore, to better visualize the effects of the infill patterns, the tensile samples printed in cylindrical form. Additionally, small cylinders produced, and diameter and height measurements taken, allowing geometric accuracy and shrinkage rates to be calculated. According to the results, the highest stress value was determined in the Grid pattern as 17.65 MPa, and the highest strain value was determined in the Hilbert Curve pattern 0.0886 mm/mm. It was also noted that samples with spiral-like infill patterns exhibited a different tendency in their tensile behavior. Finally, the greatest volumetric shrinkage calculated as 5.04% in the grid pattern.

1. INTRODUCTION

Additive manufacturing methods have become very popular due to their advantages such as enabling the production of parts with complex geometry in a single process and minimizing the amount of waste after production [1]., the method is important for material savings and light weighting, as it allows for the production of hollow parts. Depending on the type of consumables used, the method categorized into three: solid-, liquid-, and powder-based. Among these methods, FDM (Fused Deposition Modeling), which operates on the principle of extruding filament-formed thermoplastics under heat, is suitable for both personal and industrial use [2]. FDM is one of the most preferred 3D printing methods because it has many advantages such as printing without odor/smoke, ease of application, low costs and accessibility [3]. In addition to personal use for hobby purposes, its use has become widespread in many areas such as aviation, automotive, sculpture, clothing, etc. [4, 5]. Studies on the method are becoming more frequent so that it could compared with parts produced by traditional manufacturing methods.

Many parameters such as production speed, printing temperature, part orientation, layer thickness, support assignment, fill rate and internal structure geometry directly affect the surface quality, geometric accuracy and mechanical properties of the produced part. [6]. For this reason, studies on the optimization of production parameters continue intensively with the aim of improving print quality [7–13]. In the FDM method, where material-parameter matching is also important, the infill ratio and geometry are the main parameters that directly affect the material strength. [14, 15]. Software programs used for print preparation offer users a variety of options for determining void percentages and assigning geometry.

License: CC BY-NC 4.0

Therefore, numerous studies exist in the literature specifically on internal structure geometry selection for the FDM method.

Fernandez et al. investigated the infill ratio and geometry in FDM printing of ABS material. Their results indicated that the infill amount was the parameter that most significantly affected the strength value. They also achieved the highest strength in infill prints with a honeycomb pattern [16]. In another study, researchers examined the effects of infill pattern and layer thickness on the mechanical properties of materials. They observed a 75% decrease in strength values for ABS with a 0.02 mm increase in layer thickness. They also concluded that increasing the infill ratio to 50% resulted in a 25% increase in strength for ABS. [17]. In their study, Birosz et al. investigated the mechanical properties of samples with three different internal patterns made of PLA using a three-point bending test. They chose Grid, Groid, and Honeycomb patterns. According to their results, they determined that the Honeycomb and Gyroid patterns exhibited better mechanical properties than the others [18]. Alloyaydi et al. investigated the effects of different infill geometries on impact strength and low-speed compression test results. They determined that the infill pattern had an impact on mechanical properties. They explained that using a triangular pattern yielded better results than other geometries because it contained more contact points per unit area. They observed that the higher the frequency of contact points, the better the material properties. [19]. In their study, Garg et al. conducted a comprehensive investigation by combining 16 different filler patterns and 5 different filler densities. To determine mechanical properties, they applied tensile tests, microhardness measurements, and surface deformation, and also performed finite element analysis. As a result, they showed that increasing filler density increased strength and that there was a 12% difference between the simulation and experimental studies [20]. Another study investigated the effects of different infill patterns on compressive strength. The highest compressive strength achieved in the Hilbert curve pattern. The researchers also found that compressive strength increased with increasing infill ratio. Finally, they explained that surface roughness decreased as the infill ratio decreased. [21]. Tanveer et al. investigated the effects of infill density and pattern on energy absorption during deformation. They found that samples produced with a concentric pattern had very low energy storage capacity and were brittle [15]. In another study, researchers investigated the effects of different filling patterns on the flexural performance of PLA materials. By applying static and dynamic bending tests, they ultimately determined that samples with a concentric pattern yielded the best results [22]. Rudrakotti et al. produced PETG polymer samples with three different infill patterns using filament extrusion and they compared mechanical properties and surface roughness. They concluded that samples produced with a rectilinear pattern had the highest mechanical properties. Furthermore, both rectilinear and grid patterns yielded the best results in terms of surface roughness [23].

PLA is the most commonly used filament in extrusion-based 3D printers because it has many advantages such as being biodegradable and biocompatible, easy to extrude, and economical. [24]. For this reason, it is highly preferred in 3D productions in biomedical studies [1, 25]. However, due to its low mechanical properties and thermal stability compared to other thermoplastics and its brittle structure, studies carried out on the optimization of printing parameters [26]. Hamoud et al. compared the mechanical properties of PLA/Cu composite materials by subjecting samples produced in five different patterns: cross, grid, line, and tri-hexagon, to tensile testing. They determined that the pattern with the highest strength at 90% fill rate was line [27]. In another study, tensile tests conducted on PLA samples produced in cubic, gyroid, and rectilinear patterns. In the test, the highest tensile strength value for samples at 80% fill was 21.06 MPa for the cubic pattern, while the lowest value was 20.53 MPa for the gyroid pattern [1]. Dave et al., using tensile samples produced with PLA using an FDM printer, examined the variables of the infill pattern, infill ratio, and sample orientation. They concluded that as infill density increases, strength increases, and the highest tensile strength values obtained in samples with a flat, concentric pattern [28]. In another study, Birosz and Ando produced PLA materials with FDM and compared grid and honeycomb infill patterns, and as a result, they revealed that the honeycomb pattern was more durable [29].

A literature review revealed that infill patterns frequently studied in 3D printed samples produced using the FDM method. Many of these studies focused on PLA material. However, the studies concluded that all printed tensile samples produced in sheet form. Because sheet production is closer to 2D, this study used cylindrical samples. Considering the generally used thickness of approximately 3.2 mm in

standards, when an outer wall of type 2 is selected, the thickness of the inner filling pattern remains at 0.8 mm with a 0.2 mm layer thickness. In this case, the thickness covered by the inner filling pattern can be reduced to 2.4 mm. Therefore, it is not possible to clearly see the effects of the inner filling on the mechanical properties. Although comments are made about the filling density, the pattern geometry also directly affects the material strength. To see this effect more clearly, conducting tests with larger volumetric samples will allow for a more accurate comparison. It anticipated that the effects of infill patterns be more clearly seen with cylindrical samples. The study aimed to conduct a comprehensive comparison by producing tensile samples with 11 different patterns and ASTM D638 Type I standard. Since a standard for dumbbell-shaped polymer tensile specimens could not be reached, the dimensions used for dog-bone shape specimens in this study were used as a basis, and cylindrical specimens were produced by revolving the design. Additionally, to determine shrinkage amounts, prints taken for each pattern to 10 mm diameter and 20 mm height dimensions, and the geometric accuracy of the production measured with a micrometer.

2. MATERIALS AND METHOD

Esun PLA+ filament was chosen for sample printing. Prints were made on a Bambu Lab X1E-combo FDM-type 3D printer. Printing was performed using a 0.2 mm layer thickness and standard quality. Printing parameters are listed in Table 1. Infill ratio is 50% for all patterns.

A print speed of 200 mm/s chosen as a high value. This is because new model FDM printers strive to stand out in the market by offering high-speed printing capabilities. While these printers are capable of printing speeds up to 800-1000 mm/s, the default print speed is generally given as 200 mm/s. To keep up with high-speed printing technologies, the test samples printed at 200 mm/s, which is considered an average speed for new machines.

Table 1. Printing Parameters

Nozzle Diameter and Material	**0.4 mm and bronze**
Temperature	Nozzle: 230 °C, Bed: 60 °C
Bed Type	Textured PEI Plate
Quality	Standard
Layer Height	0.2 mm
Seam Position	Aligned
Wall Loops	2
Print Speed	200 mm/s wall, 270 mm/s infill
Top Shell Layers	None
Top Surface Pattern	None
Bottom Shell Layers	3
Bottom Surface Pattern	Monotonic
Bottom Layers Thickness	35 mm
Top Layers Thickness	35mm
Infill Density	50%
Infill Pattern	Variable

Eleven different infill patterns were used in the study. These include Gyroid, Archimedean Chords, Honeycomb, Concentric, Grid, Tri-hexagon, Cubic, Rectilinear, Octagram Spiral, Triangles, and Hilbert Curve. Images of the selected infill patterns provided in Figure 1. Bambu Studio version 1.10.1.50 used as slicer software. To compare strength properties, tensile tests were performed using the Utest (100 kN) Universal Tensile Tester at the Duzce University Laboratories at a deformation rate of 5 mm/min, in accordance with ASTM D638 standards. Attached extensometer is used for measurement of strain value with 50 mm gagle length. Tests repeated three times, and the average recorded.

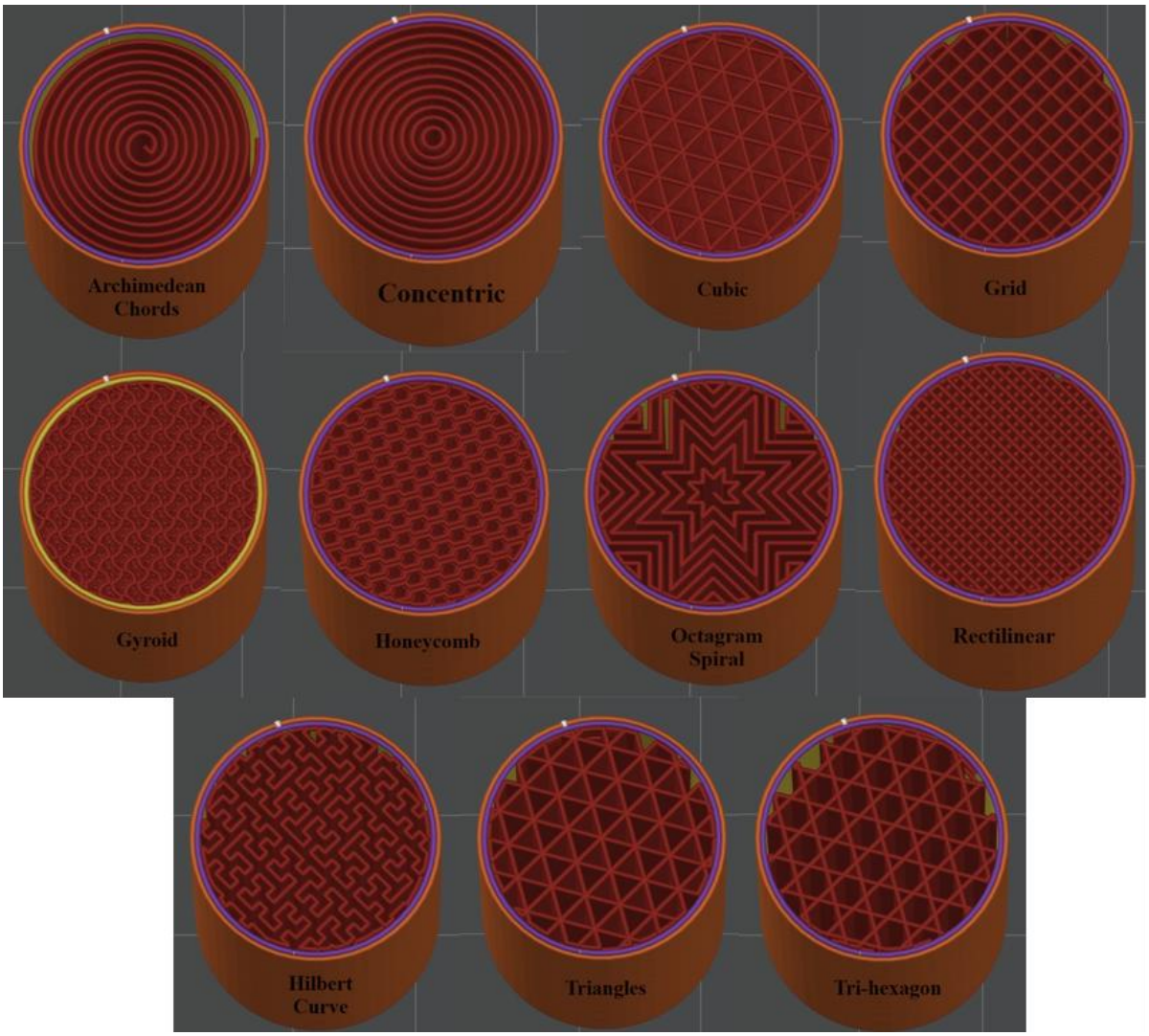


Figure 1. Infill patterns

The samples were prepared with a 50% void space as specified. This void ratio can lead to crushing during connection to the gripping jaws of the tensile testing machine. Crushing that may occur during jaw clamping will also directly affect the test results. To avoid this error, the sections to be clamped by the jaws were printed with 100% fullness, 35 mm from the bottom and 35 mm from the top. A preview of the print is given in Figure 2.

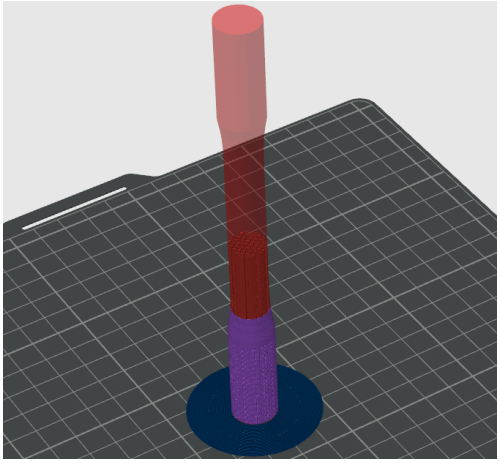


Figure 2. 3D preview of tensile test specimen after slicing.

Additionally, diameter and height measurements taken using a Mahr digital micrometer, shown in Figure 3, to verify dimensional accuracy.



Figure 3. Digital micrometer.

3. RESULTS AND DISCUSSION

The results of the tensile test performed to determine the mechanical properties are given in Figure 4 as a stress-strain graph, comparing 11 different infill patterned samples.

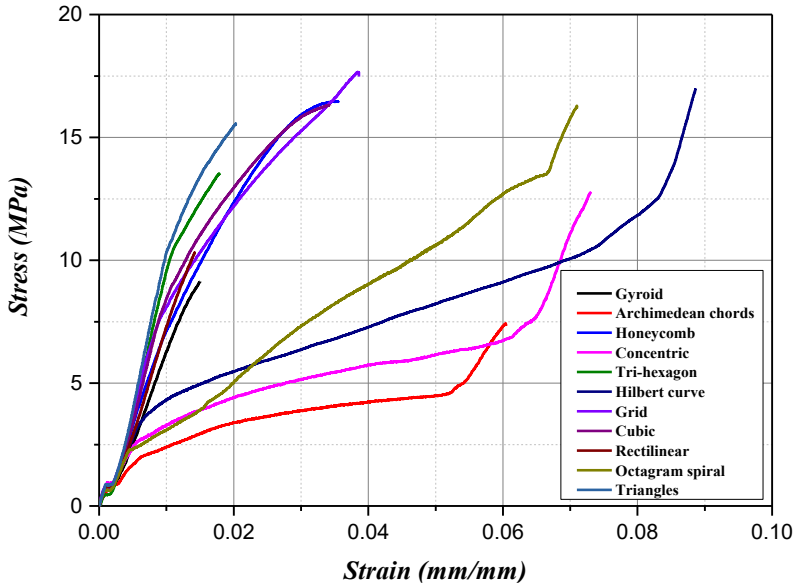


Figure 4. Comparative display of tensile test results

According to the results, the highest tensile strength was found in the Grid pattern specimens at 17.65 MPa, while the lowest was found in the Archimedean Chords pattern specimens at 7.42 MPa. When strain values were compared, the highest value was found in the Hilbert Curve pattern specimen at 0.08 mm/mm, and the lowest value was found in the Rectilinear pattern specimen at 0.0142 mm/mm. The maximum stress and strain values obtained for each specimens given in Table 2.

Table 2. Tensile test results.

Pattern	Max. Stress (MPa)	Max. Strain (mm/mm)
Gyroid	9.129	0.015
Archimedean Chords	7.436	0.0604
Honeycomb	16.463	0.0356
Concentric	12.743	0.073
Tri-Hexagon	13.534	0.0178
Hilbert Curve	16.959	0.0886
Grid	17.65	0.0385
Cubic	16.307	0.0343
Rectilinear	10.3115	0.0142
Octagram Spiral	16.279	0.071
Triangles	15.561	0.0203

Since the experiments performed in sets of three replicates, the standard deviations between the replicates are given in Table 3.

Table 3. Standard deviations of repeated experiments.

Pattern	SD for stresses	SD for Strains
Gyroid	2.578	0.0008
Archimedean Chords	0.16	0.0052
Honeycomb	0.0393	0.0008
Concentric	0.0631	0.002
Tri-Hexagon	0.326	0.0005
Hilbert Curve	0.1505	0.0033
Grid	0.428	0.0024
Cubic	0.3238	0.0068
Rectilinear	0.024	0.0004
Octagram Spiral	0.6487	0.065
Triangles	0.6585	0.0033

A notable feature of the results were the graphs in interlocking, repeating patterns within a spiral structure. These patterns can be listed as Archimedean Chords, Concentric, Hibert Curve, and Octagram Spiral. Tensile graphs for these patterns are also provided in Figure 5.

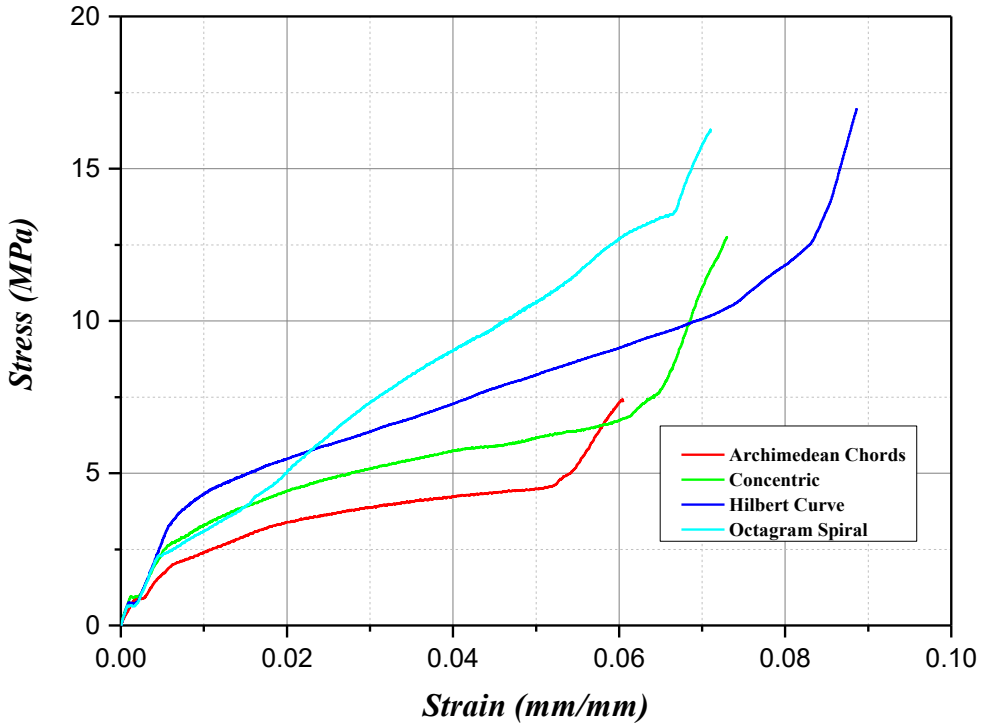


Figure 5. Tensile graphics of samples with spiral like pattern.

The fracture patterns observed in these four samples also differ from those of the other samples. While the other samples were split in two at a certain level, the spiral-like pattern showed separation on the outer wall of the samples, but the inner spiral structure remained attached, and the samples did not split into two. Fracture photographs are provided in Figure 6.



Figure 6. Test specimens of spiral like patterns after fractures

Measurement samples were printed to verify geometric accuracy and calculate the shrinkage ratio. Two samples were produced from each pattern, and diameter and height measurements were precisely made with a micrometer. Images of the printed measurement samples are shown in Figure 7.



Figure 7. Samples with diameter and height measurements checked.

According to the results, the greatest diameter shrinkage, 2.71%, was observed in samples with Hilbert Curve patterns. Furthermore, considering the order, the greatest diameter shrinkage was found in samples with spiral-like patterns. In height measurements, the largest difference, 1.01%, was also observed in the Hilbert Curve. The average of the measurements for all samples is presented in Table 4. Volume equation for cylinder used for calculations and given below.

$$V = (\pi r^2).h \tag{1}$$

Table 4. Measurement results with shrinkage ratio.

Pattern	Diameter (mm)	Height (mm)	% vol. change (Shrinkage ratio)
Gyroid	9.798	20.107	-3.49
Archimedean Chords	9.762	20.05	-4.47
Honeycomb	9.84	20.059	-2.89
Concentric	9.808	20.048	-3.57
Tri-Hexagon	9.79	20.025	-4.04
Hilbert Curve	9.729	20.196	-4.42
Grid	9.749	20.064	-5.04
Cubic	9.848	20.041	-2.82
Rectilinear	9.843	20.017	-3.03
Octagram Spiral	9.808	20.077	-3.43
Triangles	9.838	20.094	-2.76

As seen in the table, volumetric shrinkage was detected in all samples. When shrinkage rates (% volume change) were calculated, the highest shrinkage was 5.04% in grid-patterned samples.

4. CONCLUSION

The aim of this study was to investigate the effects of different infill patterns on the strength and shrinkage of FDM-printed parts. Furthermore, studies in the literature conducted using sheet-form tensile specimens. Therefore, tensile test specimens produced in cylindrical form, allowing the effects of the infill pattern to more clearly observe. Therefore, tensile specimens produced in cylindrical form and with 11 different infill patterns. To determine geometric accuracy, 3D printing of measurement specimens with a diameter of 10 mm and a height of 20 mm performed. PLA, the most commonly used thermoplastic material, chosen for this study. The results obtained from the tensile tests and dimensional measurements listed below.

- The lowest strength value was obtained as 7.436 MPa with the Archimedean Chords pattern, while this value increased to 17.65 MPa with the Grid pattern. Based on this result, it can be concluded that the part strength can be increased by approximately 42% by changing the internal filling pattern.
- When the strain results were compared, the lowest value was obtained with the Rectilinear pattern at 0.0142 mm/mm, and the highest value was obtained with the Hilbert Curve pattern at 0.0886 mm/mm. As a result, it is seen that the amount of strain can be increased by approximately 16% by changing the inner filling pattern.
- Tensile tests revealed high strength in Grid, Honeycomb, Cubic, and Triangle patterns. This is due to the density of contact points in the inner pattern. Considering the force distributions on the free-body diagram, the greater distribution and minimal force concentration with more than two contact points could attributed to the high strength.
- When comparing the internal filling patterns, it can be said that the increase in contact points within the pattern and between the pattern and the outer wall increases the strength. Considering the free-body diagrams of the internal patterns, the amount of division of the total resultant force increases with the increase in connections. In this case, since the concentration of force will be less, the force carried during the tensile test is higher in triangular-based and multi-contact internal patterns.
- Another noteworthy point in the strength tests was that the test graphs of samples with spiral-like, interlocking, repeating patterns, such as Octagram Spiral, Hilbert Curve, Concentric, and Archimedean Chords, exhibited different trends. After the outer wall reached maximum stress and ruptured, the sample did not break in two; the tensile test continued, and the force continued to transmitting to the inner pattern. This attributed to the increased force-carrying capacity due to the force's movement along the spiral structure. Because in these interior designs, when the sample is printed, the contact between the exterior wall cladding and the design occurs at a single point. Therefore, the exterior wall and the design carry the force separately. When the maximum force that the wall can withstand exceeded, cracking occurs in the wall. However, despite the cracking of the wall, the force continued to spread along the spiral in the interior filling, thus an increase in strength values observed.
- The highest strain values also determined in samples with spiral-like patterns. The high elongation is likely due to the presence of structures in these patterns where the fiber direction is parallel to the tensile axis.
- Finally, the geometric measurements of the prints precisely performed with a micrometer, and shrinkage was calculated. The greatest volumetric shrinkage observed in the grid-patterned samples as 5.04%, which also yielded the highest strength values. A general comment regarding these measurements is that the higher the density of the inner pattern, the lower the shrinkage rate.

Statement of Research and Publication Ethics

The study is complied with research and publication ethics.

Artificial Intelligence (AI) Contribution Statement

This manuscript was entirely written, edited, analyzed, and prepared without the assistance of any artificial intelligence (AI) tools. All content, including text, data analysis, and figures, was solely generated by the authors.

REFERENCES

[1] J. J. Fekiač, L. Kakošová, M. Krbata, M. Kohutiar, M. Eckert, Z. Studeny, and A. Dubec, "Influence of Infill Geometry and Density on the Mechanical Properties of 3D-Printed Polylactic Acid Structure," *Journal of Manufacturing and Materials Processing*, vol. 9, no. 4, p. 134, 2025. doi: 10.3390/JMMP9040134.

[2] M. Q. Tanveer, M. Suhaib, and A. Haleem, "A Retrospective Investigation of Mechanical and Physical Properties of ABS Specimen Developed by Manual Injection Moulding and Fused Deposition Modelling," in *Lecture Notes in Mechanical Engineering*, pp. 965–978, 2021. doi: 10.1007/978-981-15-5463-6_85.

[3] S. H. Masood, "Advances in Fused Deposition Modeling," in *Comprehensive Materials Processing*, vol. 10, pp. 69–91, 2014. doi: 10.1016/B978-0-08-096532-1.01002-5.

[4] M. Silva, I. S. Pinho, J. A. Covas, N. M. Alves, and M. C. Paiva, "3D printing of graphene-based polymeric nanocomposites for biomedical applications," *Functional Composite Materials*, vol. 2, no. 1, pp. 1–21, 2021. doi: 10.1186/S42252-021-00020-6.

[5] X. Chen, C. Gao, J. Jiang, Y. Wu, P. Zhu, and G. Chen, "3D printed porous PLA/nHA composite scaffolds with enhanced osteogenesis and osteoconductivity in vivo for bone regeneration," *Biomedical Materials*, vol. 14, no. 6, p. 065003, 2019. doi: 10.1088/1748-605X/AB388D.

[6] A. K. Sood, R. K. Ohdar, and S. S. Mahapatra, "Parametric appraisal of mechanical property of fused deposition modelling processed parts," *Materials & Design*, vol. 31, no. 1, pp. 287–295, 2010. doi: 10.1016/J.MATDES.2009.06.016.

[7] M. Daly, M. Tarfaoui, M. Chihi, and C. Bouraoui, "FDM technology and the effect of printing parameters on the tensile strength of ABS parts," *The International Journal of Advanced Manufacturing Technology*, vol. 126, no. 11, pp. 5307–5323, 2023. doi: 10.1007/S00170-023-11486-Y.

[8] T. Yao, Z. Deng, K. Zhang, and S. Li, "A method to predict the ultimate tensile strength of 3D printing polylactic acid (PLA) materials with different printing orientations," *Composites Part B: Engineering*, vol. 163, pp. 393–402, 2019. doi: 10.1016/J.COMPOSITESB.2019.01.025.

[9] P. Wang, B. Zou, S. Ding, L. Li, and C. Huang, "Effects of FDM-3D printing parameters on mechanical properties and microstructure of CF/PEEK and GF/PEEK," *Chinese Journal of Aeronautics*, vol. 34, no. 1, pp. 236–246, 2021. doi: 10.1016/J.CJA.2020.05.040.

[10] J. Kechagias and S. Zaoutsos, "Effects of 3D-printing processing parameters on FFF parts' porosity: outlook and trends," *Materials and Manufacturing Processes*, vol. 39, no. 7, pp. 804–814, 2024. doi: 10.1080/10426914.2024.2304843.

[11] S. Bardiya, J. Jerald, and V. Satheeshkumar, "The impact of process parameters on the tensile strength, flexural strength and the manufacturing time of fused filament fabricated (FFF) parts," *Materials Today: Proceedings*, vol. 39, pp. 1362–1366, 2021. doi: 10.1016/J.MATPR.2020.04.691.

[12] J. M. Gardner et al., "Machines as Craftsmen: Localized Parameter Setting Optimization for Fused Filament Fabrication 3D Printing," *Advanced Materials Technologies*, vol. 4, no. 3, p. 1800653, 2019. doi: 10.1002/ADMT.201800653.

[13] S. Palanisamy et al., "Effect of Process Parameters and Material Selection on the Quality of 3D Printed Products by Fused Deposition Modeling (FDM): A Review," *Advances in Polymer Technology*, vol. 2024, Art. no. 3480281, 2024. doi: 10.1155/ADV/3480281.

[14] M. Daly, M. Tarfaoui, M. Bouali, and A. Bendarma, "Effects of Infill Density and Pattern on the Tensile Mechanical Behavior of 3D-Printed Glycolyzed Polyethylene Terephthalate Reinforced with Carbon-Fiber Composites by the FDM Process," *Journal of Composites Science*, vol. 8, no. 4, p. 115, 2024. doi: 10.3390/JCS8040115.

[15] M. Q. Tanveer, G. Mishra, S. Mishra, and R. Sharma, "Effect of infill pattern and infill density on mechanical behaviour of FDM 3D printed Parts- a current review," *Materials Today: Proceedings*, vol. 62, pp. 100–108, 2022. doi: 10.1016/J.MATPR.2022.02.310.

[16] M. Fernandez-Vicente, W. Calle, S. Ferrandiz, and A. Conejero, "Effect of Infill Parameters on Tensile Mechanical Behavior in Desktop 3D Printing," *3D Printing and Additive Manufacturing*, vol. 3, no. 3, pp. 183–192, 2016. doi: 10.1089/3DP.2015.0036.

[17] A. Rodríguez-Panes, J. Claver, and A. M. Camacho, "The Influence of Manufacturing Parameters on the Mechanical Behaviour of PLA and ABS Pieces Manufactured by FDM: A Comparative Analysis," *Materials*, vol. 11, no. 8, p. 1333, 2018. doi: 10.3390/MA11081333.

[18] M. T. Birosz, D. Ledenyák, and M. Andó, "Effect of FDM infill patterns on mechanical properties," *Polymer Testing*, vol. 113, p. 107654, 2022. doi: 10.1016/J.POLYMERTESTING.2022.107654.

[19] B. Aloyaydi, S. Sivasankaran, and A. Mustafa, "Investigation of infill-patterns on mechanical response of 3D printed poly-lactic-acid," *Polymer Testing*, vol. 87, p. 106557, 2020. doi: 10.1016/J.POLYMERTESTING.2020.106557.

[20] Garg, A. Singh, and Q. Murtaza, "Measuring the Impact of Infill Pattern and Infill Density on the Properties of 3D-Printed PLA via FDM," *Journal of Materials Engineering and Performance*, vol. 34, no. 19, pp. 22597–22610, 2025. doi: 10.1007/S11665-025-10837-Y.

[21] P. Yadav, A. Sahai, and R. S. Sharma, "Strength and Surface Characteristics of FDM-Based 3D Printed PLA Parts for Multiple Infill Design Patterns," *Journal of The Institution of Engineers (India): Series C*, vol. 102, no. 1, pp. 197–207, 2020. doi: 10.1007/S40032-020-00625-Z.

[22] A. R. B. Rudrakotti et al., "The impact of infill patterns on the mechanical and surface characteristics of PETG material in 3D printing," *AIP Conference Proceedings*, vol. 3192, no. 1, 2024. doi: 10.1063/5.0241970.

[23] U. K. Komal, B. K. Kasaudhan, and I. Singh, "Comparative Performance Analysis of Polylactic Acid Parts Fabricated by 3D Printing and Injection Molding," *Journal of Materials Engineering and Performance*, vol. 30, no. 9, pp. 6522–6528, 2021. doi: 10.1007/S11665-021-05889-9.

[24] T. A. Son, P. S. Minh, and T. T. Do, "Effect of 3D Printing Parameters on the Tensile Strength of Products," *Key Engineering Materials*, vol. 863, pp. 103–108, 2020. doi: 10.4028/WWW.SCIENTIFIC.NET/KEM.863.103.

[25] S. Ali, I. Deiab, and S. Pervaiz, "State-of-the-art review on fused deposition modeling (FDM) for 3D printing of polymer blends and composites: innovations, challenges, and applications," *The International Journal of Advanced Manufacturing Technology*, vol. 135, no. 11, pp. 5085–5113, 2024. doi: 10.1007/S00170-024-14820-0.

[26] M. Murariu and P. Dubois, "PLA composites: From production to properties," *Advanced Drug Delivery Reviews*, vol. 107, pp. 17–46, 2016. doi: 10.1016/J.ADDR.2016.04.003.

[27] M. Hamoud, A. B. Elshalakany, M. Gamil, and H. Mohamed, "Investigating the influence of 3D printing parameters on the mechanical characteristics of FDM fabricated (PLA/Cu) composite material," *The International Journal of Advanced Manufacturing Technology*, vol. 134, no. 7, pp. 3769–3785, 2024. doi: 10.1007/S00170-024-14313-0.

[28] H. K. Dave, N. H. Patadiya, A. R. Prajapati, and S. R. Rajpurohit, "Effect of infill pattern and infill density at varying part orientation on tensile properties of fused deposition modeling-printed poly-lactic acid part," *Proceedings of the Institution of Mechanical Engineers, Part C: Journal of Mechanical Engineering Science*, vol. 235, no. 10, pp. 1811–1827, 2021. doi: 10.1177/0954406219856383.

[29] M. T. Birosz and M. Andó, "Effect of infill pattern scaling on mechanical properties of FDM-printed PLA specimens," *Progress in Additive Manufacturing*, vol. 9, no. 4, pp. 875–883, 2023. doi: 10.1007/S40964-023-00487-8.